Acute nutrient regulation of the unfolded protein response and the integrated stress response in cultured rat pancreatic islets

Short title: “H. Elouil et al.: Acute nutrient regulation of islet UPR and ISR"

H. Elouil[1], M. Bensellam[1], Y. Guiot[2], D. Vander Mierde[3], S.M.A. Pascal[1], F.C. Schuit[3], and J.C. Jonas[1]

From [1] the Unit of Endocrinology and Metabolism and [2] the Service of Pathology, Faculty of Medicine, Université catholique de Louvain, Brussels, Belgium, and [3] the Gene Expression Unit, Department of Molecular Cell Biology, Katholieke Universiteit Leuven, Leuven, Belgium.

Address correspondence to : Jean-Christophe Jonas, Unit of Endocrinology and Metabolism, Université catholique de Louvain, Avenue Hippocrate, 55 (UCL 55.30), B-1200 Brussels, Belgium.

Tel: +32 2 764 95 75

Fax: +32 2 764 55 32

E-mail: JONAS@ENDO.UCL.AC.BE

Accepted for publication in Diabetologia on March 5, 2007.

ABSTRACT

Aims/Hypothesis: Inadequate chaperone function relative to client protein load in the endoplasmic reticulum (ER) triggers an adaptive Unfolded Protein Response (UPR) including the Integrated Stress Response (ISR), the latter being also activated by other types of stresses. It is well established that pancreatic beta-cells, which synthesize and secrete insulin upon nutrient stimulation, are markedly affected by pathological disruption or excessive activation of the UPR. However, whether and how physiological nutrient stimulation affects the beta-cell UPR has been little investigated.

Methods: We compared the effects of increasing glucose concentrations and of ER Ca^{2+} emptying with thapsigargin on the UPR (*xbp1* mRNA splicing and XBP1/ATF6-target gene expression) and ISR (eIF2α phosphorylation, ATF4 protein levels and target gene expression) in isolated rat islets.

Results: Thapsigargin strongly increased both UPR and ISR. In comparison, glucose moderately increased the UPR between 5 and 30 mmol/l, but exerted complex effects on the ISR: a marked reduction between 2 and 10 mmol/l, and a moderate increase parallel to the UPR between 10 and 30 mmol/l. These glucose effects occurred within 2h, were mimicked by other metabolic substrates, but were independent from changes in Ca^{2+} influx or insulin secretion. Remarkably, attenuating the glucose stimulation of protein synthesis with a low concentration of cycloheximide prevented UPR activation but not ISR reduction by high glucose.

Conclusions/Interpretation: Nutrient stimulation acutely activates rat islet UPR in a protein synthesis-dependent manner while exerting complex effects on the ISR. These effects may contribute to nutrient-induced maintenance of the beta-cell phenotype.

Keywords: beta-cell, ER stress, gene expression, succinic acid, amino acids, α-ketoisocaproate.

ABBREVIATIONS

ATF, Activating Transcription Factor ; BiP, immunoglobulin heavy chain Binding Protein; CHX, cycloheximide; EDEM, ER-Degradation Enhancer Mannosidase α-like 1; eIF2α, eukaryotic Initiation Factor 2 subunit α ; ER, Endoplasmic Reticulum; ERAD, ER-Associated Degradation; FAM-VAD-fmk, carboxyfluorescein derivative of benzyloxycarbonyl-Val-Ala-Asp-fluoromethyl ketone; GADD, Growth Arrest and DNA Damage; Gn, n mmol/l glucose; GRP, Glucose Regulated Protein; IRE, Inositol requiring; ISR, Integrated Stress Response; SAM, Succinic Acid Monomethyl ester; PERK, Pancreatic ER Kinase; SERCA, Sarco-Endoplasmic Reticulum Ca^{2+}-ATPase; TBP, TATA-box Binding Protein; TG, thapsigargin; UPR, Unfolded Protein Response; XBP, X-box Binding Protein.

INTRODUCTION

Folding of proteins destined to the secretory pathway in the endoplasmic reticulum (ER) critically depends on adequate production and function of ER chaperones such as BiP (HSPA5), GRP94 (HSP90B), calnexin, calreticulin and protein disulfide isomerase [1]. When ER chaperone function decreases or ER client protein load increases (following ER Ca^{2+} emptying, ATP depletion, increased protein synthesis...), the Unfolded Protein Response is activated. This transiently reduces protein synthesis, improves the cell capacity to fold proteins and degrade unfolded proteins, and increases cellular defences against various types of stresses [2-4]. This response, which is controlled by the ER stress sensors IRE1 (Inositol requiring 1), ATF6 (Activating Transcription Factor 6) and PERK (Pancreatic ER Kinase), is made of two branches. The first branch results from the unconventional splicing of *X-box binding protein 1* (*xbp1*) pre-mRNA by IRE1 with subsequent increase in active XBP1, and from the proteolytic activation of ATF6. Both transcription factors contribute to increase the production of ER chaperones such as BiP and GRP94, and of components of the ER-associated degradation pathway like EDEM (ER degradation-enhancer mannosidase α-like 1) [5]. The second branch results from the phosphorylation of the eukaryotic initiation factor 2 α subunit (eIF2α) on Ser^{51} by PERK, followed by general translational pause with selective increase in *atf4* mRNA translation and subsequent stimulation of expression of ATF4-target genes like *atf3*, *gadd153, gadd34* and *bip* [6]. Because eIF2α-Ser^{51} can also be phosphorylated by other kinases (PKR, GCN2 and HRI) independently from UPR activation, events downstream from eIF2α-Ser^{51} phosphorylation (the shared branch of the UPR as defined by Ma et al. [7]) will be referred to as the "Integrated Stress Response (ISR)" regardless of the kinase involved [7-9].

Pancreatic beta-cells, which synthesize and secrete insulin in a glucose concentration-dependent manner [10], produce high levels of several UPR and ISR components.

Surprisingly, both genetic disruption and excessive activation of the UPR and ISR induce beta-cell apoptosis and insulin-dependent diabetes ([11-14], recently reviewed in [4]), suggesting that beta-cell survival and function critically depend on a continuous physiological activation of the UPR to cope with their high rate of proinsulin synthesis. More recently, it was also demonstrated that prolonged exposure to palmitate or high glucose concentrations triggers an ER stress response in insulin-secreting INS1 cells [15-17], suggesting that ER stress may play a role in beta-cell gluco-lipotoxicity in type 2 diabetes.

Glucose is the main physiological regulator of protein synthesis in beta-cells. As such, it can be expected to activate the UPR and ISR to compensate for an increase in ER client protein load. In support of that hypothesis, it was recently demonstrated that glucose acutely induces IRE1α phosphorylation and UPR activation in isolated mouse islets [18]. However, these effects were not accompanied by *xbp1* mRNA splicing, a hallmark of UPR activation [19]. In contrast, it has recently been shown that glucose rapidly decreases eIF2α phosphorylation and the ISR in MIN6 cells [20,21]. To investigate whether and to what extent physiological nutrient stimulation affects the UPR in normal beta-cells, we tested the effects of increasing glucose concentrations and of other metabolic substrates on the UPR and ISR in cultured rat islets, and compared these effects to those of the specific inhibitor of Sarco-Endoplasmic Reticulum Ca^{2+}-ATPases (SERCAs) thapsigargin (TG), a potent inducer of ER-stress in many cell types [3].

MATERIALS AND METHODS

Materials - Thapsigargin (TG), cycloheximide (CHX), succinic acid monomethyl ester (SAM), α-ketoisocaproate (KIC), L-glutamine, and diazoxide were purchased from Sigma (St Louis, MO, USA). L-leucine was from Calbiochem (San Diego, CA, USA).

Antibodies – Rabbit polyclonal anti-GADD153 (sc-575), anti-ATF4 (sc-200) and anti-XBP1 (sc-7160) antibodies were from Santa Cruz Biotechnologies (Santa Cruz, CA, USA). Mouse anti-BiP antibody (clone 40) was from BD Biosciences (San Diego, CA, USA). Rabbit polyclonal anti-ACTIN antibody was from Sigma. Mouse monoclonal anti-total-eIF2α antibody was provided by D. Scheuner, University of Michigan. Rabbit anti-phospho-eIF2α antibodies were generated as described [20].

Islet isolation and culture - Islets were isolated from the pancreas of ~200g male Wistar rats (local animal facility), as described [22]. They were precultured for 1wk at 37°C, in the presence of 5% CO_2, in serum-free RPMI-1640 medium (Gibco, Grand Island, NY, USA) containing 10 mmol/l glucose (G10), 5 g/l BSA fraction V (Roche, Basel, Switzerland), 100 IU/ml penicillin, and 100 μg/ml streptomycin. Large islets (diameter > 150 μm) were discarded. After preculture, islets were further cultured in medium containing 2-30 mmol/l glucose (G2, G5, G10 or G30) and various test substances, and collected for further analysis. All experiments were conducted in accord with accepted standards of humane animal care and were approved by the local Institutional Committee on Animal Experimentation.

RNA extraction and cDNA synthesis - Islet total RNA was extracted and reversed transcribed in cDNA as described [22].

Measurement of xbp1 mRNA splicing - cDNAs corresponding to the unspliced (*xbp1u*) and spliced (*xbp1s*) forms of *xbp1* mRNA (NM_001004210) were amplified simultaneously with TATA-box binding protein (*tbp*) cDNA by duplex radioactive PCR [19,22] (Electronic Supplement Table 1). The *spliced* over *total xbp1* mRNA ratio was calculated as an indicator of *xbp1* mRNA splicing.

Real-time fluorescent PCR - Real-time PCR was performed as described ([23] and Electronic Supplement Table 2). Within each PCR, sample threshold cycles were compared to a standard curve prepared by serial 4-fold dilutions of an appropriate control cDNA. Relative changes in gene mRNA levels were expressed relative to the mRNA levels in control islets and normalized for relative changes in *tbp* mRNA levels.

Western blotting – After rinsing with ice-cold phosphate-buffered saline (PBS), islets were precipitated with trichloracetic acid and their proteins solubilized in Laemmli buffer. For eIF2α phosphorylation measurements, islet protein extracts were prepared as described [20]. Proteins were separated by 8-12% SDS-PAGE and electrophoretically transferred to nitrocellulose membranes. The membrane was blocked (5% non-fat dry milk in Tris-buffered saline (TBS, pH 7.4) containing 0.05% Tween-20), incubated overnight with the primary antibody, washed, incubated 1h with a HRP-conjugated anti-rabbit or anti-mouse antibody, and washed before detection of bound antibodies by enhanced chemiluminescence. Band intensities were quantified by scanning densitometry and normalized to Rouge Ponceau staining intensity.

GADD153 immunohistochemistry - Islets were washed, fixed in 1% formaldehyde and embedded in paraffin. Then, GADD153 was detected on 5µm-thick sections using anti-

GADD153 antibody diluted 1/800 and the same procedure as that described previously for heme oxygenase 1 immunodetection [22].

Measurement of protein biosynthesis – Islet protein synthesis was estimated from the incorporation of L-[3,5-^{3}H]-tyrosine (Amersham Biosciences, Buckinghamshire, UK) in total islet protein extracts during culture, as previously described [24].

Insulin secretion measurements - Insulin concentrations in the culture media were determined by RIA using rat insulin as a standard [25]. The amount of insulin secreted during the whole culture period was expressed in ng.islet^{-1}.h^{-1}.

Data analysis - The results are presented as means ± SEM for the indicated number of experiments. In all cases, gene mRNA and protein levels were expressed relative to the level measured in the group of islets that had been maintained under the same condition as during the last 24h of preculture (most frequently G10).

RESULTS

Most experiments were carried out in islets precultured for 1wk in serum-free RPMI medium containing 10 mmol/l glucose (G10) and 5 g/l BSA. These islets, which have recovered from the stress of isolation [26], have a well preserved morphology and beta-cell glucose responsiveness with low level of beta-cell apoptosis [27], in marked contrast with islets cultured for several days in G5 [28]. They express *total xbp1*, *bip* and *grp94* mRNA at much higher levels than *tbp*, and *edem*, *atf3*, *gadd153* and *gadd34* mRNA at similar or lower levels (Electronic Supplement Table 2).

Effects of TG and increasing glucose concentrations on the UPR and the ISR in isolated islets – We first tested the effects of an 18h culture in the presence of 10^{-8}-10^{-6} mol/l TG. As shown in Fig. 1, TG dose-dependently increased insulin secretion, *xbp1* mRNA splicing and mRNA levels of *bip*, *grp94*, *edem*, *atf3*, *gadd153* (*chop*) and *gadd34*, without affecting *total xbp1* and *tbp* mRNA levels. TG also significantly increased islet XBP1, ATF4, BiP and GADD153 protein levels (Fig. 2), the latter being detected in most islet cell nuclei (Fig. 2**e**). The increase in *xbp1* mRNA splicing was maximal within 2h while *gadd153* mRNA levels steadily increased during the first 8h of TG treatment (data not shown). Thus, emptying ER Ca^{2+} with TG rapidly and strongly activates both UPR and ISR in rat islet cells.

We next tested the effects of a decrease or increase in glucose concentration. As shown in Fig. 1, 18h culture in G2-G5 vs. G10 resulted in a significant decrease in insulin secretion and *xbp1* mRNA splicing, the latter being always significantly higher than zero (P<0.0001 by one sample t-test). There were no changes in *total xbp1*, *grp94*, *edem* and *tbp* mRNA levels, and a strong increase in *atf3*, *gadd153*, and *gadd34* mRNA levels. The latter effect only partly resulted from a ~2.3-fold increase in *atf3* and *gadd153* mRNA half-life in G2 vs. G10 (Electronic Supplement Fig. 1). Under these conditions, XBP1 protein levels decreased in G5

vs. G10 while BiP and GADD153 protein levels increased in both G5 and G2 (Fig. 2). In G2, GADD153 increased in most islet cell nuclei (Fig. 2**c**). Clear increases in *bip* mRNA and ATF4 protein levels were only observed in G2 vs. G10 (Fig. 1**f** and 2**a-b**). Thus, lowering glucose from G10 to G2-G5 attenuates the UPR while increasing ISR gene mRNA and protein levels.

In contrast with the culture in low glucose, 18h culture in G30 vs. G10 induced a significant increase in insulin secretion, *xbp1* mRNA splicing and XBP1 protein levels without changes in *total xbp1* and *tbp* mRNA levels (Fig. 1, right panels and Fig. 2**a-b**). High glucose also induced a small similar increase in *bip*, *grp94*, *edem*, *atf3*, *gadd153* and *gadd34* mRNA levels (Fig. 1**f**, **h**). Under these conditions, culture in G30 vs. G10 significantly increased BiP but neither ATF4 nor GADD153 protein levels (Fig. 2**b**). When the islets were cultured for 1wk in G10 or G30 immediately after isolation, the *spliced/total xbp1* mRNA ratio was also significantly increased (from 0.18 ± 0.03 in G10 to 0.24 ± 0.02 in G30, n=7, $P<0.05$ by unpaired t-test). Thus, increasing glucose from G10 to G30 for 18h up to 1wk moderately activates the UPR and increases ISR gene mRNA levels in cultured rat islets.

Altogether, these results suggest that, in contrast with TG that strongly increases both UPR and ISR, glucose moderately increases the UPR between G5 and G30 but exerts complex effects on the ISR: a marked reduction from G2 to G10, and a moderate increase parallel to the UPR from G10 to G30. The effects of glucose on *xbp1* mRNA splicing and *gadd153* mRNA levels were similar in medium containing 10% FCS instead of BSA (data not shown).

Time-dependence of the effects of glucose on the UPR – We next tested the kinetics of UPR regulation by glucose between G5 and G30. After 18h culture in G5, the rate of insulin secretion and the level of *xbp1* mRNA splicing were low. Upon stimulation with G30, the

increase in insulin secretion rate and *xbp1* mRNA splicing were maximal within 2h of stimulation (Fig. 3**a-b**). In comparison, *bip* and *grp94* mRNA levels did not increase before 4-8h, while *edem* mRNA levels only rose after 24h in G30 (data not shown). Conversely, in the reverse protocol, lowering glucose from G30 to G5 led to a rapid decline in insulin secretion and *xbp1* mRNA splicing (Fig. 3**c-d**).

Time-dependence of the effects of glucose on the ISR – We also tested the kinetics of ISR regulation by glucose. After culture in G10, lowering glucose to G2 triggered a rapid increase in *gadd153* mRNA levels (Fig. 4**a**). Under these conditions, a 2h culture in G2 increased eIF2α-Ser^{51} phosphorylation to a lesser extent than addition of 10^{-6} mol/l TG in G10, whereas culture in G5 and G30 had no effect (Fig. 4**b**). Of note, eIF2α phosphorylation was never below detection limit, even after culture in G10 (the present study and [20]). These results confirm that lowering glucose from G10 to G2 acutely induces the ISR. To further document the opposite effects of glucose on islet UPR and ISR, we also measured *gadd153* mRNA levels and eIF2α-Ser^{51} phosphorylation under conditions leading to a rapid increase in *xbp1* mRNA splicing (see Fig. 3**a-b**). After 18h culture in G5, stimulation with G30 led to a rapid decrease in *gadd153* mRNA levels (Fig. 4**c**). Under these conditions, the ratio of phosphorylated/total eIF2α was significantly reduced by 2h culture in G30 vs. G5, and increased by 2h treatment with TG (Fig. 4**d**). The good parallelism between glucose-induced early changes in islet eIF2α phosphorylation and *gadd153* mRNA levels under these various conditions supports the hypothesis that culture in low glucose induces eIF2α phosphorylation and downstream activation of the ISR.

Role of mitochondrial metabolism, Ca^{2+} influx and insulin secretion – Glucose stimulation of beta-cells increases glycolysis and mitochondrial metabolism, leading to a rise in cytosolic ATP/ADP ratio, subsequent closure of ATP-dependent K^+ channels, plasma membrane

depolarization and opening of voltage-dependent Ca^{2+} channels. The resulting increase in cytosolic Ca^{2+} concentration is the triggering signal for exocytosis [10]. Except for changes in glycolysis, these stimulus-secretion coupling events can be elicited by various mitochondrial substrates in the presence of a non stimulatory glucose concentration [29,30]. As shown in Table 1, addition of a combination of 5 mmol/l leucine and 5 mmol/l glutamine (Leu-Gln), 10 mmol/l succinic acid monomethyl ester (SAM) or 5 mmol/l α-ketoisocaproate (KIC) to G5 stimulated insulin secretion and *xbp1* mRNA splicing while reducing *gadd153* mRNA expression, SAM and KIC being as effective as G10. Thus, the effects of glucose on islet UPR and ISR are reproduced by various metabolic substrates that bypass glycolysis.

To evaluate the role of plasma membrane depolarization, stimulation of Ca^{2+} influx and insulin secretion, we tested the effects of diazoxide, a drug that reduces Ca^{2+} influx and insulin secretion by opening ATP-dependent K^+ channels [10]. As expected, addition of diazoxide to G10 and G30 significantly reduced insulin secretion. However, it did not alter *xbp1* mRNA splicing nor *gadd153* mRNA levels (Table 1). Similar results were obtained when insulin secretion was inhibited by clonidine, an α_2-adrenergic agonist that inhibits cAMP production [31] and uncouples exocytosis from the rise in cytosolic Ca^{2+} concentration [32](data not shown). Thus, glucose activates the UPR and reduces the ISR independently from its effects on beta-cell membrane potential, Ca^{2+} influx and insulin secretion.

Role of protein synthesis - Acceleration of mitochondrial metabolism by glucose and other metabolic substrates rapidly stimulates beta-cell protein synthesis with a preferential effect on proinsulin [33,34]. To investigate the role of changes in ER client protein load in the glucose regulation of the UPR and ISR, we tested the effect of cycloheximide (CHX), an inhibitor of protein synthesis. Under control conditions, islet protein synthesis was markedly increased between G2 and G10 and slightly decreased between G10 and G30 (Fig. 5**a**, open circles).

CHX dose-dependently inhibited protein synthesis in G10 with a half-maximal effective concentration of ~0.1 μmol/l (data not shown). At that concentration, CHX did not affect islet protein synthesis in G2, but reduced it in G5, G10 and G30 (Fig. 5**a**, closed circles). This attenuation of the glucose-stimulation of protein synthesis completely prevented the glucose stimulation of *xbp1* mRNA splicing, *bip*, *grp94* and *edem* mRNA expression (Fig. 5**c-f**), but affected neither glucose-induced insulin secretion (Fig. 5**b**) nor glucose–induced reduction in *atf3, gadd153* and *gadd34* mRNA levels (Fig. 5**g-h** and data not shown). In contrast, CHX failed to reduce the stimulation of *xbp1* mRNA splicing triggered by TG in G10 while completely preventing the increase in *bip* mRNA levels (Electronic supplement Fig. 2**a-b**). After 1 day culture in G5, CHX also completely prevented the stimulation of *xbp1* mRNA splicing triggered by 2h culture in G30 without counteracting the reduction in *gadd153* mRNA levels (Electronic supplement Fig. 2**c-d**). Thus, reducing the glucose stimulation of protein synthesis, hence of ER protein load, abrogates the glucose stimulation of islet UPR while leaving unaffected the reduction of the ISR.

DISCUSSION

This study demonstrates that stimulation of isolated rat islets with glucose and other nutrients induces a rapid and sustained activation of the Unfolded Protein Response, the maximal intensity of which is less than that induced by 10^{-7} mol/l TG. Thus, like TG, glucose rapidly increases *xbp1* mRNA splicing (a specific marker of IRE1 and UPR activation [19]) and XBP1 protein levels without increasing *total xbp1* mRNA levels. This effect is unrelated to the stimulation of Ca^{2+} influx and insulin secretion, but likely results from the stimulation of protein synthesis in beta-cells. Thus, glucose-induced UPR activation was unaffected by diazoxide or clonidine, but was abrogated by CHX at a concentration that did not suppress protein synthesis but only prevented its stimulation by glucose (Fig. 5**a**). Although the CHX-mediated reduction in the mRNA levels of UPR-responsive genes (*bip*, *grp94* and *edem*) may result from reduced synthesis of UPR transcription factors, the decrease in *xbp1* mRNA splicing can unambiguously be attributed to a reduction in IRE1 activity upon inhibition of protein synthesis. Thus, CHX fails to inhibit *xbp1* mRNA splicing in response to TG treatment, indicating that IRE1, when adequately stimulated, is still able to splice *xbp1* pre-mRNA in CHX-treated islets. Our results therefore strongly suggest that activation of the UPR by high glucose results from an increase in ER client protein load (Fig. 6**b**). The observation that *xbp1* mRNA splicing never reaches zero even after culture at low glucose suggests that the basal rate of protein synthesis in G2 is sufficient to slightly activate the UPR in cultured rat islets.

Our results slightly contrast with a recent study showing that glucose increases IRE1α phosphorylation and UPR gene expression without increasing *xbp1* mRNA splicing in isolated mouse islets [18]. This discrepancy is unlikely due to species differences, because glucose increases *xbp1* mRNA splicing in mouse islets under our culture conditions (M. Bensellam, unpublished results). It may rather result from the use of freshly isolated vs.

precultured islets, since *xbp1* mRNA splicing was significantly higher in fresh vs. cultured rat islets (spliced/*total xbp1* mRNA ratio : 0.55 ± 0.02 in fresh islets vs. 0.20 ± 0.01 in1wk-precultured islets, n=21-28, $P<0.0001$ by unpaired t-test). This high level of *xbp1* mRNA splicing, which may result from the stress of isolation, was observed regardless of the pre-isolation condition, thereby preventing us from studying the impact of in vivo hyperglycaemia on UPR activation.

What could be the physiological role of nutrient-activation of the UPR in islet beta-cells? Its rapid onset upon glucose stimulation and fast reduction upon lowering the glucose concentration suggest that meal-related fluctuations in plasma nutrient concentration may induce synchronous fluctuations of *xbp1* mRNA splicing and other early steps of the UPR in beta-cells. By adapting the ER chaperone to client protein ratio and the ER-associated degradation capacity to physiological variations in protein synthesis, temporal integration of these UPR fluctuations could contribute to the plasticity of the beta-cell phenotype [35]. Our hypothesis may seem at variance with the observation, by electron microscopy, of normal beta-cells in *xbp1* knockout mice with a liver-specific rescue of *xbp1* expression [36]. However, the argument is not sufficient to exclude a role for XBP1 in beta-cell plasticity for several reasons. First, because *apolipoprotein E* mRNA is expressed in rat islets (M. Bensellam, unpublished results), expression of *xbp1* under the apolipoprotein E promoter may have corrected XBP1 deficiency not only in the liver but also in beta-cells. Second, beta-cell function was not evaluated in that study, leaving open the possibility that beta-cells were defective in these mice despite their normal morphology. Third, it is possible that XBP1 is not important in the early post-natal period but becomes so later in life, when beta-cells are more responsive to nutrient stimulation.

Although we had expected that the ISR would be activated by nutrients in parallel with *xbp1* mRNA splicing as it is after TG treatment, we unexpectedly observed a partial dissociation between both responses. Thus, the UPR was low in G2-G5 and concentration-dependently activated by G10 and G30, whereas the ISR was high in G2, minimal (though different from zero) in G10, and slightly increased in G30, as shown by changes in eIF2α phosphorylation, ATF4 protein levels and ATF4-target gene mRNA levels. That low glucose strongly induces the ISR in beta-cells was also recently demonstrated in MIN6 cells [21]. As there were no detectable increases in eIF2α phosphorylation and ATF4 production in G5 vs. G10, the rise in ATF4-target gene mRNA levels in G5 may result from their transcriptional activation by a mechanism different from the ISR and from their concomitant stabilisation. Our interpretation that the ISR is activated in G5 is, however, supported by the observations that eIF2α phosphorylation rapidly decreases upon stimulation from G5 to G30 in rat islets (see Fig. 4**d**) and within the whole physiological range of glucose concentrations in MIN6 cells [20,37].

Investigating the mechanism of ISR activation in low glucose was not our aim. Our results nevertheless clearly demonstrate that it can be prevented or acutely reduced by stimulation with glucose (and SAM, KIC and Leu-Gln) independently from the stimulation of Ca^{2+} influx, insulin secretion and protein synthesis. It could result either from the activation of any eIF2α kinase, among which PERK and GCN2 are the most likely candidates [11], or by the inactivation of protein phosphatase 1, mediated by inhibitor-1 which is highly expressed in beta-cells [20]. In other cell types, complete glucose deprivation is known to induce the UPR, an effect generally attributed to ER Ca^{2+} emptying and reduced ER chaperone function at very low ATP concentrations [1,3]. However, the situation was clearly different in G2-G5, where the islet ATP/ADP ratio is only moderately reduced as compared with G10 [27,38], and *xbp1* mRNA splicing was not increased.

Although we did not fully investigate the mechanisms behind the asymmetric V-shaped glucose-concentration response curve for changes in islet ISR gene expression, our results allow us to propose the following model. On the one hand, the ISR is activated in parallel with nutrient activation of the classical UPR (pathway 1, Fig. 6**b**), as shown by the parallel increases in *xbp1* mRNA splicing and in the expression of UPR and ISR gene mRNA levels between G10 and G30. This ISR activation is very low, as neither eIF2α phosphorylation nor an increase in ATF4 or GADD153 protein expression could be detected in G30 vs. G10. The ~1.6-fold increase in ATF4-target gene mRNA levels in G30 vs. G10 is, however, compatible with our estimation (based on changes in *xbp1* mRNA splicing) that the maximal glucose activation of the UPR is less than that produced by 10^{-7} mol/l TG. On the other hand, low glucose concentrations (G2 and G5 vs. G10) rapidly increase ISR gene mRNA levels by inducing the ISR and, to some extent, by increasing ATF4-target gene mRNA stability (pathway 2, Fig. 6**b**). The reduction in ISR gene mRNA and protein levels between G5 and G10 despite concurrent activation of the UPR therefore indicates that, within that physiological range of glucose concentrations, pathway 2 predominates over pathway 1 for the regulation of the ISR (Fig. 6**b**).

What could be the role of the asymmetric V-shaped glucose concentration-dependent changes in ISR in islet beta-cells? In the short term, changes in eIF2α phosphorylation may play a role in the nutrient-regulation of protein synthesis [12,14,20,37]. This hypothesis is compatible with our finding of an inverse correlation between glucose-induced changes in islet ISR gene mRNA levels and total protein synthesis after 18h culture. It is strongly supported by the observation that inhibiting glucose-induced eIF2α de-phosphorylation markedly reduced the acute glucose-stimulation of protein synthesis in MIN6 cells [20]. In the long term, beta-cell apoptosis after 2-7 days of culture also displayed a V-shaped glucose concentration-dependent curve [27,28,39,40]. Thus, by measuring caspase activation, we confirmed that islet cell

apoptosis is minimal after 1wk culture in G10 and significantly increased by G2-G5 and, to a lesser extent, by G30 (Electronic Supplement Fig. 2). The rather good correlation between rapid ISR activation and slower induction of apoptosis reinforces the hypothesis of a causal link between both events under various conditions [13,41]. Thus, although the activation of islet ISR and apoptosis by G30 vs. G10 was rather small in comparison to that induced by low glucose, the sustained activation of the islet UPR by G30 is compatible with recent studies indicating that prolonged exposure to high glucose or high free fatty acid concentrations induces an ER stress response that may contribute to the slow deterioration of beta-cell function and survival in type 2 diabetes [15-17,42,43]. In this context, it will be of utmost importance to clarify the issue as to whether ISR activation contributes to beta-cell apoptosis [13,41,44], protects against it [45,46], or is just a marker of beta-cell exposure to pro-apoptotic stimuli.

In conclusion, our results demonstrate that nutrient stimulation of rat islets moderately activates the classical UPR in a protein synthesis-dependent manner and inhibits the strong activation of ISR gene expression induced by low glucose concentrations. Both effects lead to an asymmetric V-shaped glucose-concentration response curve for changes in islet ISR. The kinetics of these effects suggests their possible role in nutrient-induced changes of the beta-cell phenotype under both physiological and pathological conditions.

ACKNOWLEDGEMENTS

The authors thank Anne Dannau and Fabien Knockaert for expert technical help and Donalyn Scheuner (University of Michigan, Ann Arbor) for supply of the eIF2α antiserum. This work was made possible by a "Grant from the EFSD/MSD Research Partnership for European Studies on Beta Cell Function and Survival". It was supported by Grant 1.5.182.04 from the Fonds de la Recherche Scientifique (F.R.S.-FNRS, Belgium), Grants 3.4616.05 and 3.4506.05 from the Fonds de la Recherche Scientifique Médicale (Belgium), the Interuniversity Poles of Attraction Program (P5/17)-Belgian Science Policy, Grant ARC 05/10-328 from the General Direction of Scientific Research of the French Community of Belgium, and Grant (GOA/2004/11) from the KU-Leuven to FS. MB is Research Fellow and JCJ is Senior Research Associate of the FRS-FNRS (Belgium).

Duality of interest statement: The authors have nothing to disclose.

REFERENCES

1. Fink AL (1999) Chaperone-mediated protein folding. Physiol Rev 79 : 425-449

2. Ma Y, Hendershot LM (2004) ER chaperone functions during normal and stress conditions. J Chem Neuroanat 28 : 51-65

3. Schroder M, Kaufman RJ (2005) The mammalian unfolded protein response. Annu Rev Biochem 74 : 739-789

4. Marciniak SJ, Ron D (2006) Endoplasmic reticulum stress signaling in disease. Physiol Rev 86 : 1133-1149

5. Lee AH, Iwakoshi NN, Glimcher LH (2003) XBP-1 regulates a subset of endoplasmic reticulum resident chaperone genes in the unfolded protein response. Mol Cell Biol 23 : 7448-7459

6. Lu PD, Harding HP, Ron D (2004) Translation reinitiation at alternative open reading frames regulates gene expression in an integrated stress response. J Cell Biol 167 : 27-33

7. Ma Y, Hendershot LM (2004) Herp is dually regulated by both the endoplasmic reticulum stress-specific branch of the unfolded protein response and a branch that is shared with other cellular stress pathways. J Biol Chem 279 : 13792-13799

8. Harding HP, Zhang Y, Zeng H et al. (2003) An integrated stress response regulates amino acid metabolism and resistance to oxidative stress. Mol Cell 11 : 619-633

9. Jiang HY, Wek SA, McGrath BC et al. (2004) Activating transcription factor 3 is integral to the eukaryotic initiation factor 2 kinase stress response. Mol Cell Biol 24 : 1365-1377

10. MacDonald PE, Joseph JW, Rorsman P (2005) Glucose-sensing mechanisms in pancreatic β-cells. Philos Trans R Soc Lond B Biol Sci 360 : 2211-2225

11. Scheuner D, Song B, McEwen E et al. (2001) Translational control is required for the unfolded protein response and in vivo glucose homeostasis. Mol Cell 7 : 1165-1176

12. Harding HP, Zeng H, Zhang Y et al. (2001) Diabetes mellitus and exocrine pancreatic dysfunction in *Perk*-/- mice reveals a role for translational control in secretory cell survival. Mol Cell 7 : 1153-1163

13. Oyadomari S, Koizumi A, Takeda K et al. (2002) Targeted disruption of the Chop gene delays endoplasmic reticulum stress-mediated diabetes. J Clin Invest 109 : 525-532

14. Scheuner D, Vander Mierde D, Song B et al. (2005) Control of mRNA translation preserves endoplasmic reticulum function in beta cells and maintains glucose homeostasis. Nat Med 11 : 757-764

15. Kharroubi I, Ladriere L, Cardozo AK, Dogusan Z, Cnop M, Eizirik DL (2004) Free fatty acids and cytokines induce pancreatic β-cell apoptosis by different mechanisms: role of NF-κB and endoplasmic reticulum stress. Endocrinology 145 : 5087-5096

16. Wang H, Kouri G, Wollheim CB (2005) ER stress and SREBP-1 activation are implicated in β-cell glucolipotoxicity. J Cell Sci 118 (Pt.17) : 3905-3915

17. Karaskov E, Scott C, Zhang L, Teodoro T, Ravazzola M, Volchuk A (2006) Chronic palmitate but not oleate exposure induces endoplasmic reticulum stress, which may contribute to INS-1 pancreatic β-cell apoptosis. Endocrinology 147 : 3398-3407

18. Lipson KL, Fonseca SG, Ishigaki S et al. (2006) Regulation of insulin biosynthesis in pancreatic beta cells by an endoplasmic reticulum-resident protein kinase IRE1. Cell Metab 4 : 245-254

19. Calfon M, Zeng H, Urano F et al. (2002) IRE1 couples endoplasmic reticulum load to secretory capacity by processing the XBP-1 mRNA. Nature 415 : 92-96

20. Vander Mierde D, Scheuner D, Quintens R et al. (2006) Glucose activates a PP1 mediated signaling pathway to enhance overall translation in pancreatic beta cells. Endocrinology 148 : 609-617

21. Greenman IC, Gomez E, Moore CE, Herbert TP (2007) Distinct glucose-dependent stress responses revealed by translational profiling in pancreatic β-cells. J Endocrinol 192 : 179-187

22. Jonas JC, Guiot Y, Rahier J, Henquin JC (2003) Haeme-oxygenase 1 expression in rat pancreatic β-cells is stimulated by supraphysiological glucose concentrations and by cyclic AMP. Diabetologia 46 : 1234-1244

23. Elouil H, Cardozo AK, Eizirik DL, Henquin JC, Jonas JC (2005) High glucose and hydrogen peroxide increase c-Myc and haeme-oxygenase 1 mRNA levels in rat pancreatic islets without activating NFκB. Diabetologia 48 : 496-505

24. Garcia-Barrado MJ, Ravier MA, Rolland JF, Gilon P, Nenquin M, Henquin JC (2001) Inhibition of protein synthesis sequentially impairs distinct steps of stimulus-secretion coupling in pancreatic β cells. Endocrinology 142 : 299-307

25. Heding LG (1972) Determination of total serum insulin (IRI) in insulin-treated diabetic patients. Diabetologia 8 : 260-266

26. Jonas JC, Laybutt DR, Steil GM et al. (2001) High glucose stimulates early response gene c-Myc expression in rat pancreatic β cells. J Biol Chem 276 : 35375-35381

27. Khaldi MZ, Guiot Y, Gilon P, Henquin JC, Jonas JC (2004) Increased glucose sensitivity of both triggering and amplifying pathways of insulin secretion in rat islets cultured for one week in high glucose. Am J Physiol Endocrinol Metab 287 : E207-E217

28. Van de Casteele M, Kefas BA, Cai Y et al. (2003) Prolonged culture in low glucose induces apoptosis of rat pancreatic β-cells through induction of c-myc. Biochem Biophys Res Commun 312 : 937-944

29. Malaisse WJ, Sener A, Malaisse-Lagae F et al. (1982) The stimulus-secretion coupling of amino acid-induced insulin release. Metabolic response of pancreatic islets of L-glutamine and L-leucine. J Biol Chem 257 : 8731-8737

30. Malaisse WJ, Rasschaert J, Villanueva-Penacarrillo ML, Valverde I (1993) Respiratory, ionic, and functional effects of succinate esters in pancreatic islets. Am J Physiol 264 : E428-E433

31. Schuit FC, Pipeleers DG (1986) Differences in adrenergic recognition by pancreatic A and B cells. Science 232 : 875-877

32. Renstrom E, Ding WG, Bokvist K, Rorsman P (1996) Neurotransmitter-induced inhibition of exocytosis in insulin-secreting β cells by activation of calcineurin. Neuron 17 : 513-522

33. Ashcroft SJ, Bunce J, Lowry M, Hansen SE, Hedeskov CJ (1978) The effect of sugars on (pro)insulin biosynthesis. Biochem J 174 : 517-526

34. Schuit FC, In't Veld PA, Pipeleers DG (1988) Glucose stimulates proinsulin biosynthesis by a dose-dependent recruitment of pancreatic beta cells. Proc Natl Acad Sci U S A 85 : 3865-3869

35. Hinke SA, Hellemans K, Schuit FC (2004) Plasticity of the β cell insulin secretory competence: preparing the pancreatic β cell for the next meal. J Physiol 558 : 369-380

36. Lee AH, Chu GC, Iwakoshi NN, Glimcher LH (2005) XBP-1 is required for biogenesis of cellular secretory machinery of exocrine glands. EMBO J 24 : 4368-4380

37. Gomez E, Powell ML, Greenman IC, Herbert TP (2004) Glucose-stimulated protein synthesis in pancreatic β-cells parallels an increase in the availability of the translational ternary complex (eIF2-GTP.Met-tRNAi) and the dephosphorylation of eIF2α. J Biol Chem 279 : 53937-53946

38. Detimary P, Jonas JC, Henquin JC (1995) Possible links between glucose-induced changes in the energy state of pancreatic B cells and insulin release. Unmasking by decreasing a stable pool of adenine nucleotides in mouse islets. J Clin Invest 96 : 1738-1745

39. Hoorens A, Van de Casteele M, Klöppel G, Pipeleers DG (1996) Glucose promotes survival of rat pancreatic β cells by activating synthesis of proteins which suppress a constitutive apoptotic program. J Clin Invest 98 : 1568-1574

40. Efanova IB, Zaitsev SV, Zhivotovsky B et al. (1998) Glucose and tolbutamide induce apoptosis in pancreatic β-cells - A process dependent on intracellular Ca^{2+} concentration. J Biol Chem 273 : 33501-33507

41. Cardozo AK, Ortis F, Storling J et al. (2005) Cytokines downregulate the sarcoendoplasmic reticulum pump Ca^{2+} ATPase 2b and deplete endoplasmic reticulum Ca^{2+}, leading to induction of endoplasmic reticulum stress in pancreatic β-cells. Diabetes 54 : 452-461

42. Cnop M, Welsh N, Jonas JC, Jorns A, Lenzen S, Eizirik DL (2005) Mechanisms of pancreatic β-cell death in type 1 and type 2 diabetes: many differences, few similarities. Diabetes 54 (Suppl. 2) : S97-S107

43. Laybutt DR, Preston AM, Akerfeldt MC et al. (2007) Endoplasmic reticulum stress contributes to beta cell apoptosis in type 2 diabetes. Diabetologia 50 : doi :10.1007/s00125-006-0590-z

44. Hartman MG, Lu D, Kim ML et al. (2004) Role for activating transcription factor 3 in stress-induced β-cell apoptosis. Mol Cell Biol 24 : 5721-5732

45. Boyce M, Bryant KF, Jousse C et al. (2005) A selective inhibitor of eIF2α dephosphorylation protects cells from ER stress. Science 307 : 935-939

46. Yusta B, Baggio LL, Estall JL et al. (2006) GLP-1 receptor activation improves beta cell function and survival following induction of endoplasmic reticulum stress. Cell Metab 4 : 391-406

LEGENDS TO FIGURES

Figure 1. Effects of thapsigargin (TG) and increasing glucose concentrations on insulin secretion during culture (**a**, **b**), spliced/*total xbp1* mRNA ratio (**c**, **d**), and the mRNA levels of *total xbp1*, *bip*, *grp94*, *edem*, *atf3*, *gadd153 (chop)* and *gadd34* (**e-h**) in isolated rat islets. After 1wk preculture in G10, the islets were cultured 18h in G10 plus increasing TG concentrations (**a, c, e, g**) or in G2, G5, G10 and G30 (**b, d, f, h**). *Gene*/*tbp* mRNA ratios are expressed relative to the ratio in islets cultured in G10. Data are means ± SEM for 3 TG and 7 glucose experiments. * $P<0.05$ or less vs. islets cultured in G10 (one-way ANOVA + test of Newman-Keuls). § $P<0.001$ by unpaired t-test. **f, h,** # the *P* values for comparison of G30 vs. G10 mRNA levels by unpaired t-test were 0.008 for *bip*, 0.007 for *grp94*, 0.005 for *edem*, 0.036 for *atf3*, 0.003 for *gadd153* and 0.007 for gadd*34*. **h**, please note the logarithmic Y scale.

Figure 2. Effects of increasing glucose concentrations and TG on XBP1, GADD153, ATF4, BiP and ACTIN protein levels in cultured rat islets. After 1wk preculture in G10, the islets were cultured 18h in the presence of G2, G5, G10, G30 or G10 + 1 µmol/l TG. **a-b**, XBP1, GADD153, ATF4, BiP and ACTIN protein levels were measured by Western Blot as described under Methods and expressed relative to the level measured in islets cultured in G10. **c-e**, GADD153 was immunodetected on sections of islets cultured 18h in G2 (**c**), G10 (**d**) or G10 + TG (**e**). Results are representative (**a, c-e**) or means ± SEM (**b**) for 3-4 experiments. * $P<0.05$ vs. islets cultured in G10, # $P<0.05$ for the effect of G30 vs. G5 (one-way ANOVA + test of Newman-Keuls). **b**, please note the logarithmic Y scales.

Figure 3. Kinetics of glucose induced-changes in insulin secretion (**a, c**) and spliced/*total xbp1* mRNA ratio (**b, d**) in 1wk precultured islets. **a-b,** the islets were cultured 18h in G5 before being cultured in G5 (open symbols) or G30 (closed symbols) for 30min up to 24h. **c-**

d, the islets were cultured 18h in G30 before being cultured in G30 (closed symbols) or G5 (open symbols). The rate of insulin secretion was calculated over the whole culture period of each sample. Data are means ± SEM for 3-4 experiments. * P<0.05 or less vs G5 (**a-b**) or G30 (**c-d**) (one-way ANOVA + test of Dunnett).

Figure 4. Acute effects of glucose on *gadd153* mRNA levels (**a, c**) and eIF2α-Ser^{51} phosphorylation (**b, d**) in 1wk precultured islets. **a-b**, after preculture in G10, the islets were cultured in G10 (closed symbols) or G2 (open symbols) for 30min up to 24h (**a**), or for 2h in G2, G5, G10, G30 or G10 + 1 µmol/l TG (**b**). **c-d**, the islets were cultured 18h in G5 before being cultured in G5 (open circles) or G30 (closed circles) for 30 min up to 24h, (**c**) or for 2h in G5, G30 or G5 + 1 µmol/l TG (**d**). *Gadd153/tbp* mRNA ratios are expressed relative to the ratio measured in islets at time 0. The levels of phosphorylated and total eIF2α protein levels (eIF2α^{P} and eIF2α^{total} respectively) were measured by Western Blot, and the ratio eIF2α$^{P/total}$ was expressed relative to the mean ratio in G10 (**b**) or G5 (**d**). Results are means ± SEM for 3 to 4 experiments. * P<0.01 vs islets cultured in G10 (**a-b**) or G5 (**c-d**)(one-way ANOVA + test of Newman-Keuls).

Figure 5. Effects of cycloheximide (CHX) on glucose-induced changes in total protein synthesis (**a**), insulin secretion during culture (**b**), spliced/*total xbp1* mRNA ratio (**c**) and *bip*, *grp94*, *edem*, *gadd153* and *atf3* mRNA levels (**d-h**) in isolated rat islets. After 1wk preculture in G10, the islets were cultured 18h in G2, G5, G10 or G30 without (open circles) or with CHX 0.1 µmol/l (closed circles). *Gene/tbp* mRNA ratios are expressed relative to the ratio in islets cultured in G10. Data are means ± SEM for 3-4 experiments. * P<0.05 for the effects of glucose vs. G10 in the presence or absence of CHX; $^{\#}$ P<0.05 for the effect of CHX under the same condition. **g-h**, please note the logarithmic Y scales.

Figure 6. Nutrient regulation of the UPR and ISR gene mRNA levels in pancreatic beta-cells. **a**, glucose-induced changes in *xbp1* mRNA splicing (UPR) and average changes in *atf3*, *gadd153* and *gadd34* mRNA levels (ISR) relative to their level after culture in G10 (normalized data from Fig. 1 **d** and **h**). **b**, proposed model (for explanations, see discussion).

Table 1. Effects of mitochondrial metabolic substrates and diazoxide on insulin secretion during culture, *xbp1* mRNA splicing and *gadd153* mRNA expression in cultured rat islets.

	Insulin secretion *(ng.islet^{-1}.h^{-1})*	*Spliced/total xbp1* mRNA ratio	*Gadd153/tbp mRNA ratio (relative to G10)*
G5	0.26 ± 0.04	0.10 ± 0.01	8.46 ± 1.16
G5 + Leu-Gln	2.07 ± 0.27 [a]	0.15 ± 0.01 [a]	2.72 ± 0.19 [a]
G5 + SAM	2.33 ± 0.62 [a]	0.21 ± 0.03 [a]	1.20 ± 0.17 [a]
G5 + KIC	2.64 ± 0.49 [a]	0.19 ± 0.01 [a]	1.51 ± 0.13 [a]
G10	2.03 ± 0.04 [a]	0.20 ± 0.01 [a]	1.00 ± 0.09 [a]
G10 + DZ	0.39 ± 0.04 [b]	0.21 ± 0.01	0.62 ± 0.04
G30	3.38 ± 0.34 [a]	0.30 ± 0.01 [a]	1.86 ± 0.22 [a]
G30 + DZ	1.45 ± 0.20 [b]	0.33 ± 0.03 [a]	1.47 ± 0.23

After 1wk preculture in G10, the islets were cultured 18h in G5, G10 or G30 in the eventual presence of a combination of 5 mmol/l leucine and 5 mmol/l glutamine (Leu-Gln), 10 mmol/l succinic acid monomethyl ester (SAM), 5 mmol/l α-ketoisocaproate (KIC), or 50 µmol/l diazoxide (DZ), as indicated. *Gadd153/tbp* mRNA ratios are expressed relative to the ratio in islets cultured in G10. There were no significant changes in *tbp* and *total xbp1* mRNA levels. Data are means ± SEM for 3-6 experiments. [a] $P<0.05$ vs islets cultured in G5; [b] $P<0.05$ for the effect of DZ in G10 or G30 (one-way ANOVA + test of Newman-Keuls).

H. Elouil et al, figure 1

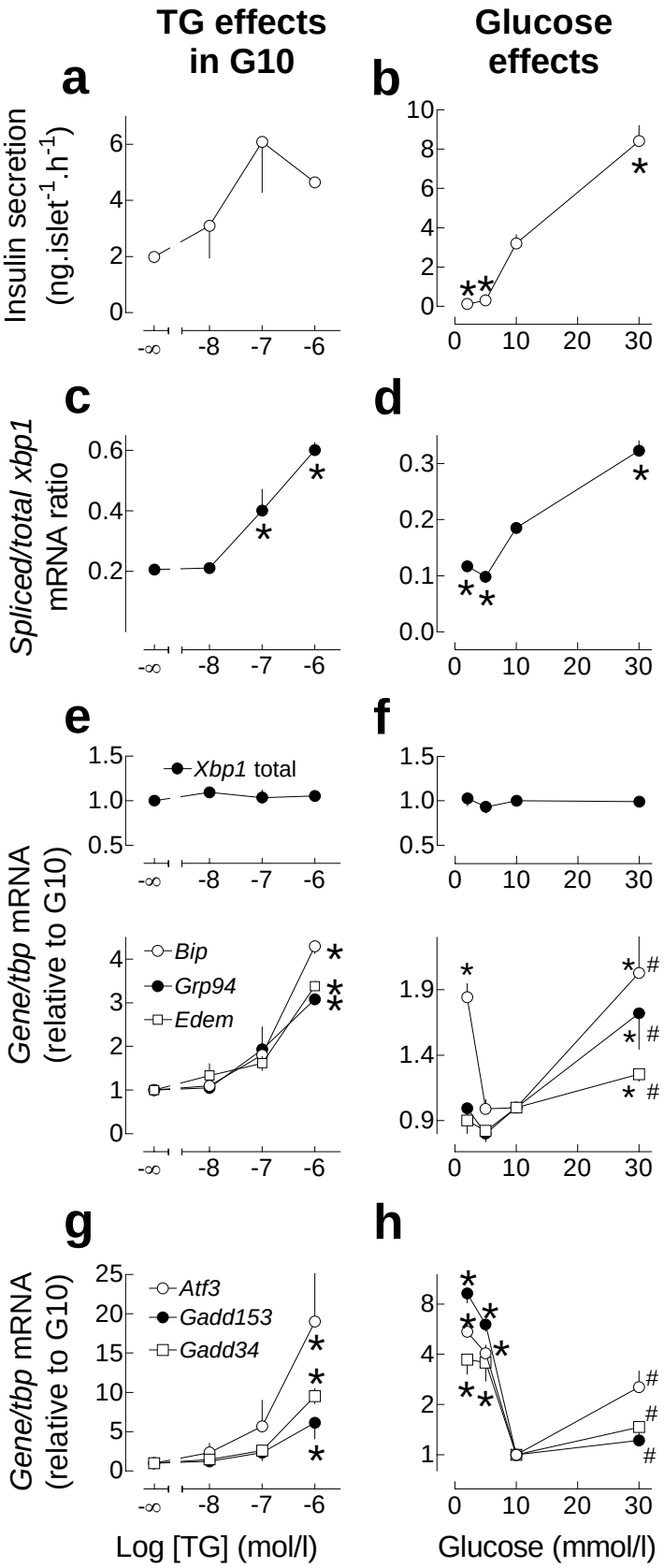

H. Elouil et al, Figure 2

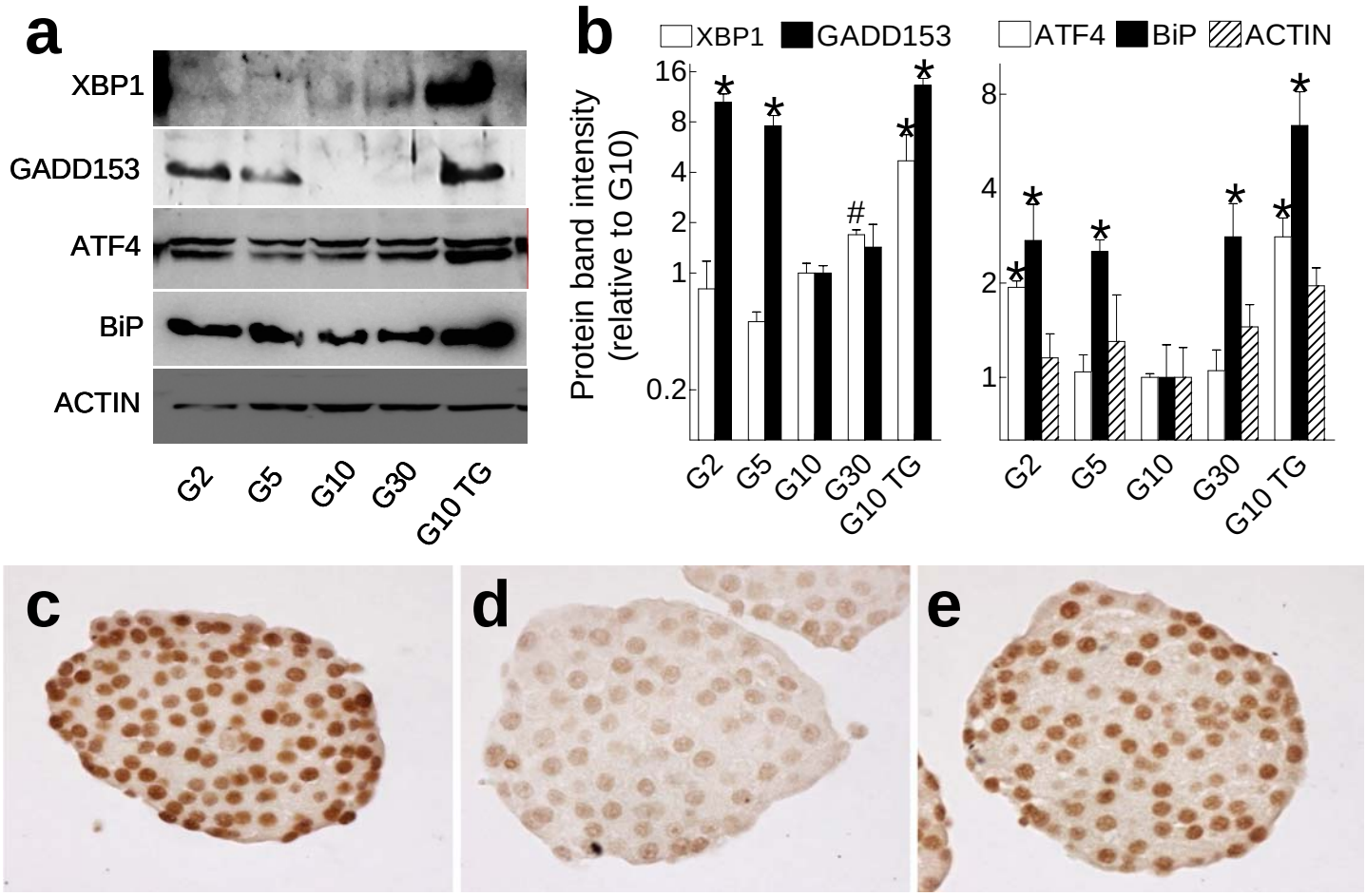

H. Elouil et al, figure 3

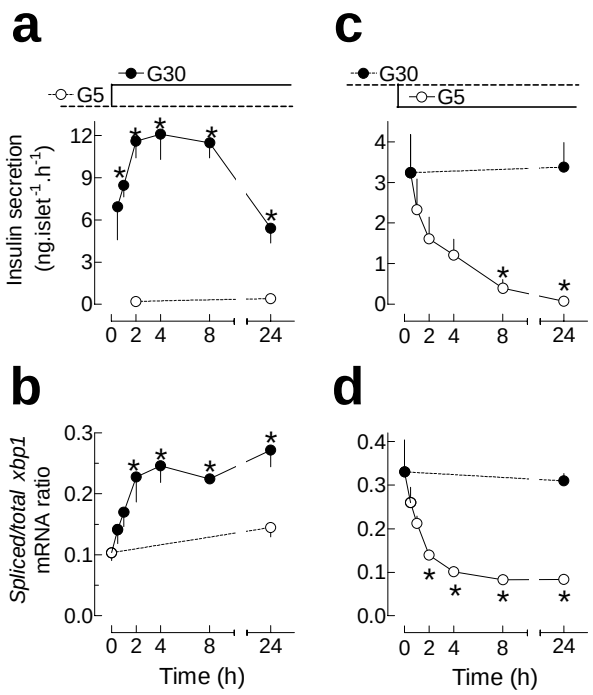

H.Elouil et al, figure 4

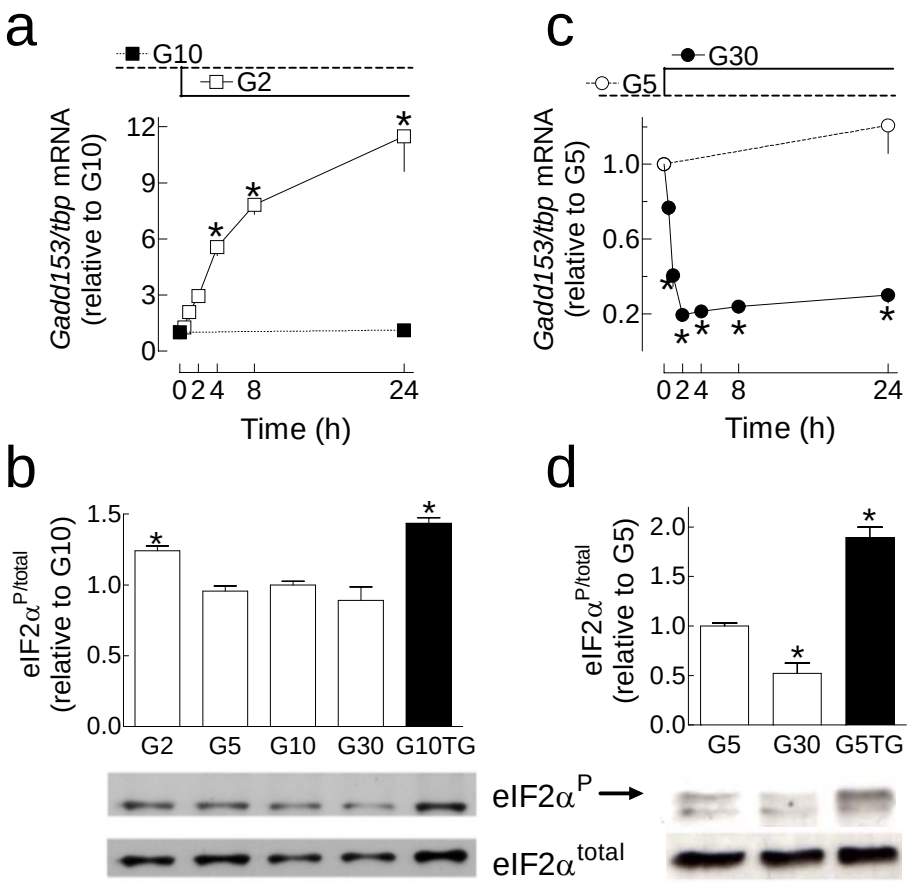

H. Elouil et al, figure 5

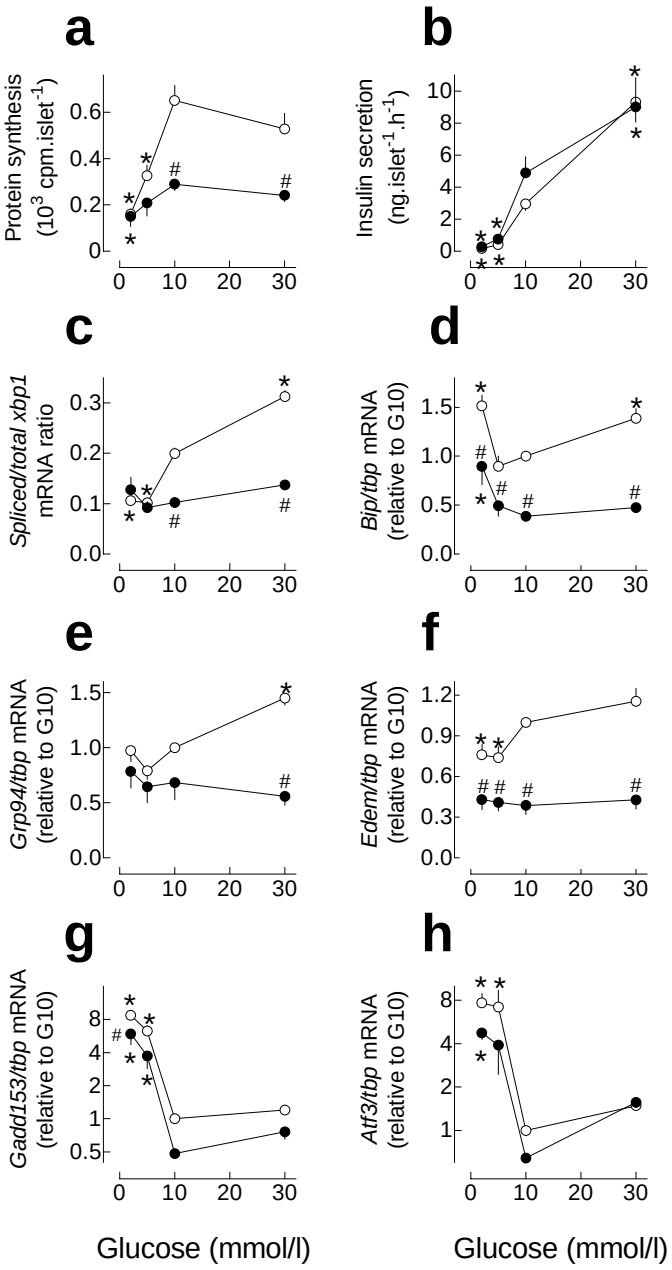

H. Elouil et al, figure 6

a

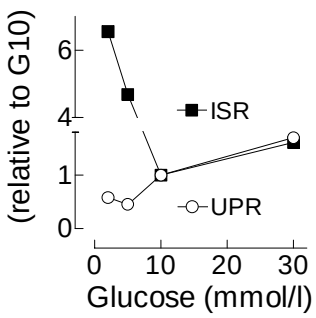

b

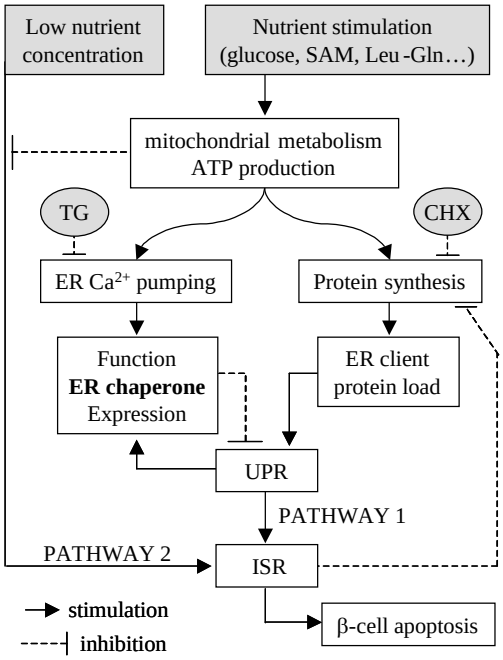

Electronic Supplement Table 1. Sequences of oligonucleotide primers and reaction conditions for radioactive multiplex PCR amplification of *xbp1s*, *xbp1u* and *tbp* cDNAs.

Gene	5'-sense primer-3'	5'-antisense primer-3'	Size (bp)
Tbp	ACC.CTT.CAC.CAA.TGA.CTC.CTA.TG	ATG.ATG.ACT.GCA.GCA.AAT.CGC	198
Xbp1u (unspliced)	CAA.GGG.GAA.TGG.AGT.AAG.GC	GAA.GAG.GCA.ACA.GCG.TCA.GA	140
Xbp1s (spliced)	CAA.GGG.GAA.TGG.AGT.AAG.GC	GAA.GAG.GCA.ACA.GCG.TCA.GA	114

The thermal cycle profile consisted of a 10 min step at 95°C to release AmpliTaq Gold DNA polymerase activity (Applied Biosystem, Foster City, CA, USA) followed by 25 cycles of amplification (60 sec denaturation step at 95°C, 60 sec annealing step at 62°C and 60 sec extension step at 72°C) and a final 10 min extension step at 72°C. The PCR products were separated by PAGE and the amount of [α-^{32}P]dCTP incorporated in each amplimer was quantified with a Cyclone Storage Phosphor System (Packard, Meriden, CT, USA). The ratio *xbp1s / (xbp1s + xbp1u)* was computed after correction for differences in dCTP incorporation between *xbp1u* and *xbp1s* amplicons. The intra-assay coefficient of variation was 5.5% for the *total xbp1/tbp* mRNA ratio and 4.8% for the *spliced/total xbp1* mRNA ratio. The mean ± SD *total xbp1/tbp* mRNA ratio in islets cultured in G10 was 14.1 ± 2.5 (n=10).

Electronic Supplementary Table 2. Sequences of oligonucleotide primers, reaction conditions for real-time PCR and characteristics of PCR products.

Gene	5'-sense primer-3'	5'-antisense primer-3'	Input [a]	Annealing (°C-sec)	Extension (°C)	Size (bp)	T_m (°C)
Tbp	ACC.CTT.CAC.CAA.TGA.CTC.CTA.TG	ACT.TCG.TGC.CAG.AAA.TGC.TGA	2	variable	variable	157	84.0
Cyclophilin	AAC.CCC.ACC.GTG.TTC.TTC	TGC.CTT.CTT.TCA.CCT.TCC.C	2	62-90	80	400	87.5
Bip (Hspa5)	TCA.GCC.CAC.CGT.AAC.AAT.CA	AAG.GTG.ACT.TCA.ATC.TGG.GGT.A	2	62-45	82	132	84.5
Grp94 (Hsp90b1)	GAG.TGT.TCA.TCA.CAG.ACG.ACT.TC	GGA.AAC.ATT.GAG.GGG.GAG.ATC	2	62-45	80	98	82.0
Edem	CCT.TGG.ATA.CAC.TCG.CAA.TAA.TGG	AAG.ACT.TGG.ACG.GTG.GAA.TCT	2	60-45	80	106	81.0
Atf3	TGC.TGC.CAA.GTG.TCG.AAA.CA	GGT.GCA.GGT.TGA.GCA.TGT.AAA.TCA	4	60-60	-	152	84.0
Gadd153 (Ddit3)	GTC.ACA.AGC.ACC.TCC.CAA.AG	CCA.CTC.TGT.TTC.CGT.TTC.CTA.G	2	62-45	80	110	83.0
Gadd34 (Ppp1r15a)	TGG.ACA.CGC.CTT.AGA.AAC.CTA.C	GGG.AGA.GGG.AGT.GGT.CA	2	61-45	81	117	86.5

The thermal cycle profile consisted of a 3min step at 95°C to release DNA polymerase activity followed by 40 cycles of amplification (15 sec denaturation step at 95°C, 45-60 sec annealing step at 60-62°C, and eventual 15 sec extension step at 79-82°C). Under these conditions, PCR efficiencies ranged from 0.95 to 1.0. The size of amplicons measured by agarose gel electrophoresis corresponded to that expected from published sequences. The specificity of amplicons was routinely verified by determination of their melting temperature (T_m) at the end of PCR. The mean ± SD (n=10) threshold cycles in islets cultured in G10 using the indicated cDNA input per 25 µL reactions ([a], ng total RNA equivalent) were : 28.4 ± 0.8 for *tbp*, 22.8 ± 0.5 for *cyclophilin*, 21.8 ± 0.9 for *bip*, 22.7 ± 0.8 for *grp94*, 26.9 ± 0.9 for *edem*, 29.2 ± 0.7 for *atf3*, 26.6 ± 0.9 for *gadd153* and 27.7 ± 0.5 for gadd*34*.

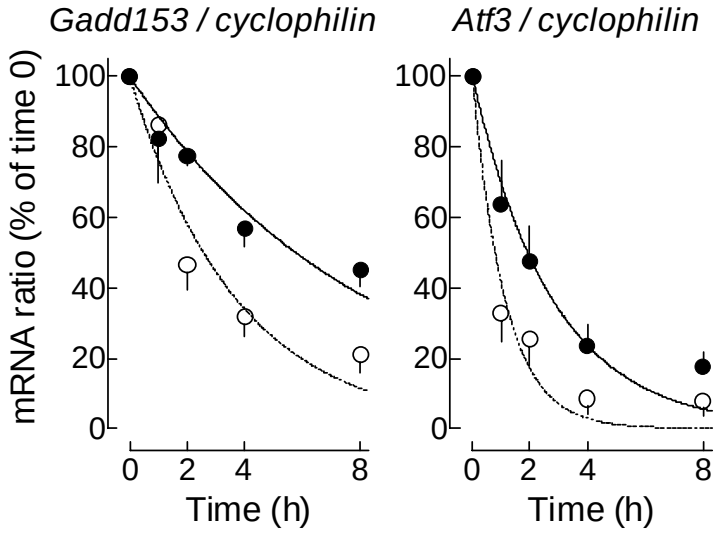

Electronic Supplement Fig. 1. Effect of glucose on *gadd153* and *atf3* mRNA half-life in cultured rat islets. After preculture, the islets were cultured 18h in G2 (closed circles) or G10 (open circles) and subsequently treated for 1 to 8h with 5 µg/ml actinomycin D under the same conditions. *Gadd153* and *Atf3* mRNA levels were normalized to *cyclophilin* rather than *tbp* mRNA levels because the latter has a short half-life [22] whereas the former remained unaffected by 8h treatment with actinomycin D. After 18h culture in G2, *gadd153*, *atf3* and *cyclophilin* mRNA levels were respectively 9.5 ± 0.5, 7.0 ± 0.1 and 1.4 ± 0.1 relative to the levels in islets cultured in G10. *Gadd153* and *atf3* over *cyclophilin* mRNA ratios are expressed in percentage of the ratio measured in each type of islets before addition of actinomycin D (time 0). The data were fitted to a one-phase exponential decay equation ($Y=Span*e^{(-K*X)} + Plateau$ where Span and Plateau are fixed at 100 and 0% respectively and half-life=0.69/K) using Graphpad Prism 4.0. The mean [95% confidence interval] half-life was ~5.8h [4.9-6.9] in G2 and ~2.6h [1.9-3.7] in G10 for *gadd153* mRNA and ~1.9h [1.5-2.6] in G2 and ~0.8h [0.6-1.1] in G10 for *atf3* mRNA ($P<0.0001$ by F-test comparing regression curves in G2 and G10). *Gadd153* mRNA was similarly stabilized after cultured in G5 but not G30 vs. G10 (data not shown). Assuming that such mRNA stabilization occurred immediately upon lowering of the glucose concentration from G10 to G2, we estimated that the increases in *gadd153* and *atf3* mRNA levels measured under these conditions also require a concurrent ~3-4-fold increase in mRNA production rate. Results are means ± SEM for 3-4 experiments.

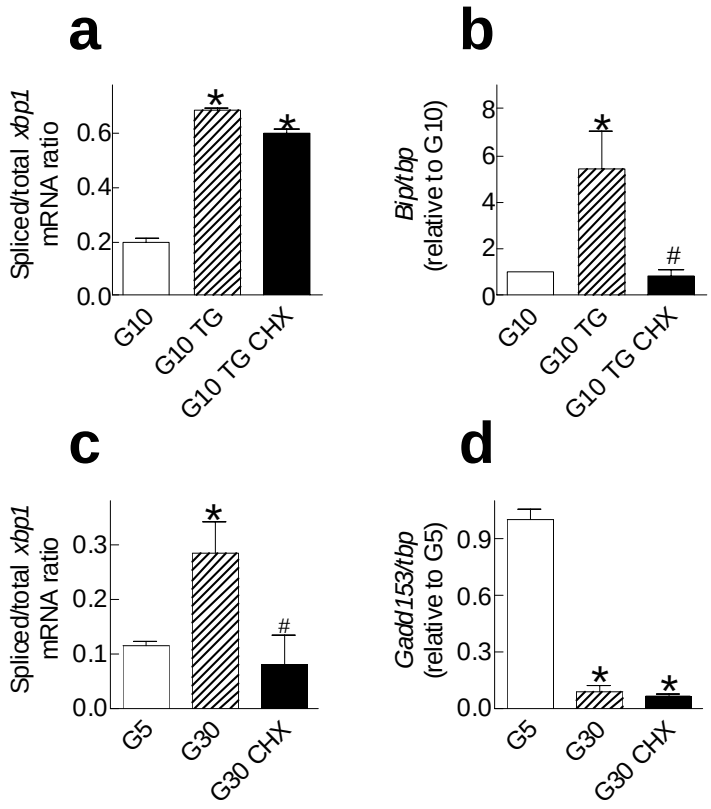

Electronic Supplement Fig. 2. Effects of cycloheximide (CHX) on glucose-and TG-induced changes in *xbp1* mRNA splicing (**a, c**), *gadd153* and *bip/tbp* mRNA ratio (**b, d**) in isolated rat islets. **a-b,** after 1wk preculture in G10, the islets were cultured 18h in G10 (white column) or G10 + 1 µmol/l TG in the absence (hatched column) or presence of 10 µmol/l CHX (black column). **c-d**, the islets were cultured 18h in G5 before being cultured for 2h in G5 (white column), G30 (hatched column) or G30 with CHX 0.1 µmol/l (black column). Gene mRNA levels are expressed relative to the levels in islets cultured in G10 (**b**) or G5 (**d**). Data are means ± SEM for 3-4 experiments. * $P<0.05$ for the effects of TG vs. G10 (**a-b**) or G30 vs. G5 (**c-d**) in the presence or absence of CHX; # $P<0.05$ for the effect of CHX under the same condition.

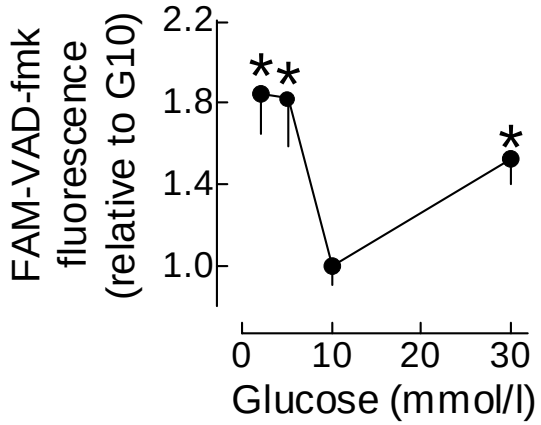

Electronic Supplement Fig. 3. Glucose-induced changes in islet caspase activation. After 1 wk culture in G2, G5, G10 or G30, islet cell apoptosis was measured with the ApoFluor™ Green Caspase Activity Detection kit (MP Biomedicals, Irvine, CA, USA) following manufacturer instructions. At the end of culture, the islets were incubated for 1h in RPMI medium containing G10 and a 1/150 dilution of FAM-VAD-fluoromethylketone dissolved in dimethylsulfoxide (DMSO). This cell-permeable fluorochrome-labeled caspase inhibitor covalently binds to the catalytic site of active caspases (caspase-1 to –9). The islets were then rinsed thrice with RPMI medium to allow diffusion of unbound FAM-VAD-fmk out of the islets. Fluorescence microscopy images of labeled islets were acquired with an Olympus IX70 inverted fluorescence microscope (20× objective) coupled to a CCD camera (T.I.L.L. photonics, Martinsried, Germany) using excitation/emission wavelengths of 490/520 nm. The islets were protected from light throughout the procedure. Caspase activation was expressed relative to its level after culture in G10. Data are means ± SEM for 5 experiments. * $P<0.05$ vs. G10 (one-way ANOVA + test of Newman-Keuls).